# STRUCTURAL PROPERTIES OF CRYSTALLINE AND POLYCRYSTALLINE CR MODELS: A MOLECULAR DYNAMIC STUDY

**Mai Van Dung**[(1)]
*(1) Thu Dau Mot University*
*Corresponding author: dungmv@tdmu.edu.vn*

**DOI: 10.37550/tdmu.EJS/2024.04.599**

## Article Info

**Volume:** 6
**Issue:** 04
**Dec** 2024
**Received:** Sep 25th, 2024
**Accepted**: Oct 21th, 2024
**Page No:** 531-539

## Abstract

In this paper, the structural properties of crystalline and polycrystalline Cr have been investigated using molecular dynamics simulations. The interaction between atoms is modeled via the MEAM potential. Periodic boundary conditions are applied in the x, y, and z directions. The structural characteristics are analyzed through the total energy function, heat capacity, radial distribution function, and angle distribution. Dynamics are evaluated through the analysis of mean squared displacement and diffusion coefficient. The results show that the melting temperature of crystalline Cr is higher than that of polycrystalline Cr, indicating that the polycrystal melts earlier. This information is important when considering material applications in high-temperature environments.

**Keywords:** crystalline, molecular; polycrystalline, structure

## 1. Introduction

Recently, novel high-temperature alloys based on headstrong metals (Perepezko, 2009; Senkov et al., 2010) have received significant attention in developing alloys besides Ni-based superalloys (HARADA et al., 1979; Long et al., 2018; Reed, 2008; Xia et al., 2020). Chromium (Cr) can be utilized as a high-temperature material due to its higher melting temperature and lower density than compared to Ni. Chromium, one of the 25 most common elements in the Earth's crust with an average abundance of 100 ppm (Emsley, 2011), is widely used in the chemical industry for various applications such as pigments, metal plating, or tanning, and in chemical production such as chemical synthesis and as a catalyst (Unceta et al., 2010). The melting point of Cr has been the subject of both theoretical and experimental studies (Bloom & Grant, 1951; Carlile et al., 1949; Greenaway et al., 1951; Grube & Knabe, 1936; Haworth & Hume-Rothery, 1959; Ioroi et al., 2022; Josell et al., 2001; Putman et al., 1951). However, these reports reveal discrepancies among the obtained results. Specifically, experimental results using thermal analysis methods indicate the melting temperature of Cr as follows: 1890 ± 10°C (Grube & Knabe, 1936) reported by Grube et al., 1860 ± 20°C (Carlile et al., 1949) published by Carlile et al., 1892°C (Putman et al., 1951) indicated by Putman et al., the melting point

of 1930°C (Bloom & Grant, 1951) revealed by Bloom et al., 1845 ± 10°C (Greenaway et al., 1951) presented by Greenaway et al., and 1903 ± 10°C (Bloom et al., 1952) published by Bloom et al. The heating method was also used by Haworth et al. to determine the melting temperature of Cr, with results showing Cr melts at 1849 ± 20°C (Haworth & Hume-Rothery, 1959), a value that aligns well with Greenaway's experimental results. In 2001, using the pulse heating technique, Josell et al. determined the melting temperature of Cr to be 1842 ± 20°C (Josell et al., 2001). This result aligns well with previous experimental results. Most recently in 2022 (Ioroi et al., 2022), Ioroi et al. used thermal analysis methods with a differential scanning calorim (Bloom et al., 1952) eter (DSC) and a differential thermal analyzer (DTA). Their results confirmed that the melting temperature of Cr is 1861 ± 3°C. This value is in good agreement with experimental results published by Josell et al. By using molecular dynamics simulation, Shibuta et al. determined the melting temperature of Cr nanoparticles containing 31250 atoms to be 2177 K (Shibuta & Suzuki, 2008). This simulation result is in line with experimental results.

Although many studies have aimed to determine the melting temperature of Cr material, however, they have not yet detailed the phase transition process of the material. Therefore, in this paper, we use molecular dynamics simulation methods to describe in detail the phase transition process of crystalline and polycrystalline Cr materials, providing more information for practical tests.

## 2. Computational method

### *2.1. Construction of Models*

The crystalline Face Centered Cubic (FCC) and polycrystalline models of Cr are described as shown in Figure 1. Both models have the same dimensions of 54 × 54 × 54 Å$^3$. FCC atoms are green, while the unknown coordination structure (Other) atoms are blue.

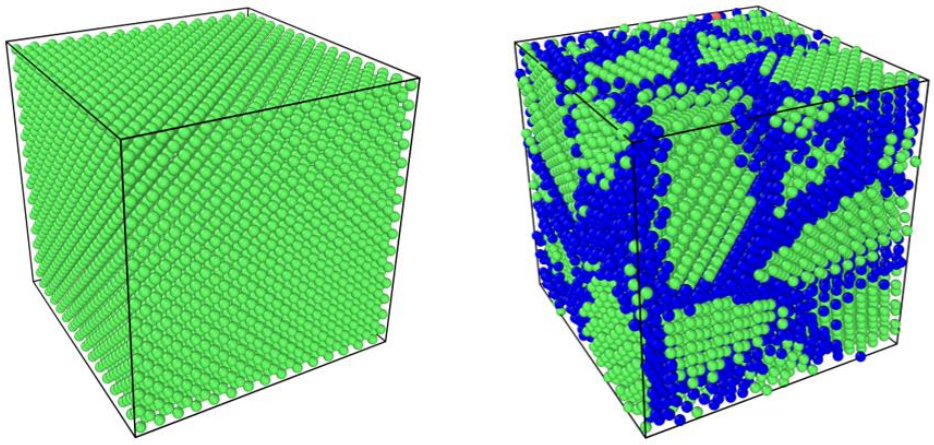

a) Crystal FCC Cr b) Polycrystal Cr

***Figure 1***. Crystalline and polycrystalline model Cr.

### *2.2. Procedures of Simulation*

In this study, the properties of Cr crystal and polycrystal systems are investigated using the Large-scale Atomic/Molecular Massively Parallel Simulator (LAMMPS) software (Plimpton, 1995). This highly reliable open-source software package is used for molecular dynamics (MD) simulations with the Verlet algorithm to approximate the equations of

motion with a time step of 0.001 ps. LAMMPS has been widely used for molecular dynamics (MD) simulations due to its ability to utilize interatomic potentials from the Interatomic Potentials Repository (NIST) and its capability to accurately describe interactions between atoms in metal and alloy material models. In this study, the interactions between atoms are carried out through the MEAM potential (Choi et al., 2017). The MEAM potential can effectively describe the structural and thermodynamic properties, fitting well with experimental data. The total energy of the MEAM potential is given by:

$$E = \sum_i \{F_i(\bar{\rho}_i) + \frac{1}{2}\sum_{i,jj\neq i} S_{ij}\emptyset_{ij}(R_{ij})\}$$

The embedding function $F_i$ represents the energy an atom $i$ receives when embedded in a background electron density $\rho_i$. The pair interaction $\Phi_{ij}$ between atoms $i$ and $j$ is multiplied by the many-body screening function $S_{ij}$, which indicates the extent to which the interaction between atoms $i$ and $j$ is screened by neighboring atoms. To investigate the structural properties and thermodynamics of Cr crystal and polycrystal systems, we proceed as follows: The initial Cr crystal and polycrystal systems are created at 300 K and equilibrated over $10^5$ time steps in the NPT ensemble ($N$ is the number of particles, $P$ is the pressure, and $T$ is the temperature) until equilibrium is reached. Periodic boundary conditions are applied in the x, y, and z directions. Then, the system, equilibrated at 300 K, is heated to 3500 K at a heating rate of $10^{12}$ K/s under a pressure of 0 GPa. To control the pressure and temperature, the Nosé-Hoover thermostat and barostat were used (Hoover, 1985; Nosé, 1984). For visualizing the model and calculating structural units using the Common Neighbor Analysis (CNA) method, we used the OVITO software (Stukowski, 2009). It should be noted that system characteristics such as the radial distribution function, mean squared displacement, diffusion coefficient, strain, and model visualizations at each temperature will be equilibrated over $10^5$ simulation steps.

## 3. Results and discussions

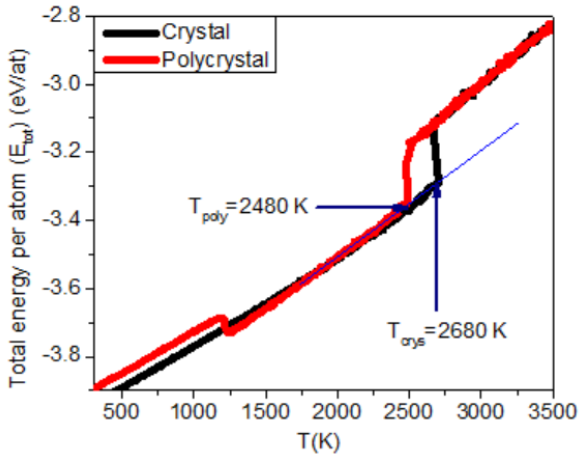


***Figure 2***. Total energy per atom for Cr crystal and polycrystal with increasing temperature

Figure 2 illustrates the total energy per atom as a function of temperature for both crystalline (black line) and polycrystalline (red line) Cr systems. The critical temperatures where phase changes or significant structural transformations occur are marked as $T_{poly}$ for the

polycrystal (2480 K) and $T_{crys}$ for the crystal (2680 K). For both the crystalline and polycrystalline, the total energy per atom increases as temperature rises, which is typical due to increased atomic vibrations and thermal motion. At approximately 2480 K, the polycrystal undergoes a noticeable change, as indicated by a discontinuity or slope change in the red curve. This suggests a phase transition, potentially from a solid to a partially molten state. Similarly, the crystal system shows a phase change at a higher temperature, around 2680 K. The sharper transition indicates a possible melting point, aligning with the properties of ordered crystal structures, which tend to melt at higher temperatures compared to polycrystalline materials. The energy of the polycrystalline system is consistently higher than that of the crystalline system. This reflects the increased defect density in polycrystals, which leads to more energy being stored within grain boundaries and dislocations, lowering its thermal stability. The graph demonstrates that polycrystalline structures are less thermally stable than their crystalline counterparts, with earlier phase transitions. This is consistent with known material behavior, where defects in polycrystals cause them to melt or transition phases at lower temperatures compared to crystals.

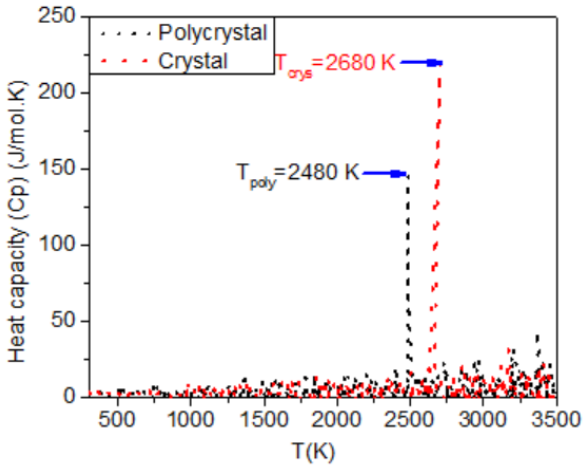


***Figure 3***. Heat capacity for Cr crystal and polycrystal models with the increase of temperature from 300 to 3500 K.

Figure 3. represents the heat capacity (*Cp*) of both the crystal and polycrystal as a function of temperature. Similar to the Figure 1, the polycrystal melts at around 2480 K, and the crystal melts at 2680 K. These temperatures are much higher compared to the results of Shibuta et al. (Shibuta & Suzuki, 2008). There are significant spikes in the heat capacity at the melting points. This is expected because, during a phase transition (such as melting), the system absorbs a large amount of heat without a corresponding increase in temperature. This results in a peak in the heat capacity. The crystal and polycrystal models exhibit similar behavior but at different temperatures. Below the melting points, both the crystal and polycrystal models have relatively low and constant heat capacities, typical for solids. The polycrystal model has a slightly higher heat capacity in the pre-melting region, indicating that it requires more energy to increase its temperature compared to the crystal model. The graphs clearly show that the polycrystal model has a lower melting temperature than the crystal model. This is typical because polycrystalline materials, with their grain boundaries, tend to melt at lower temperatures than single crystals due to structural imperfections. The energy and heat capacity behaviors suggest that the polycrystal model is thermodynamically less stable than the crystal model. The crystal model, with its more ordered structure, resists melting and maintains stability at higher temperatures.

Figure 4 displays the relationship between temperature and density for both polycrystalline and crystalline models of a material. As temperature increases, the density of both models decreases, which is a typical behavior for most solids as they expand with rising temperatures. The density of the crystalline model (red line) is higher than that of the polycrystalline model (black line) across the entire temperature range. For the polycrystal model, the melting temperature is around 2480 K while that of the crystal model is 2680 K. There is a significant drop in density at these melting points, indicating a phase transition from solid to liquid. This drop is more pronounced in the crystalline model. The lower density and melting temperature of the polycrystal model suggest that it has a more disordered structure compared to the crystalline model, which results in a weaker bonding network that requires less energy to melt. The higher stability of the crystalline structure, as evidenced by its higher melting temperature and density, suggests that it retains its ordered arrangement more effectively under increasing thermal conditions.

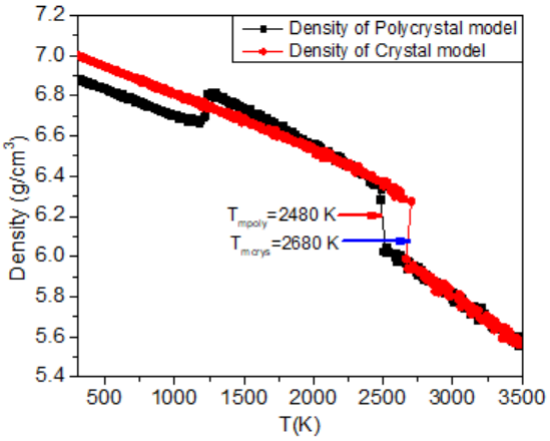


***Figure 4***. Temperature dependence of density in the crystal and polycrystal models

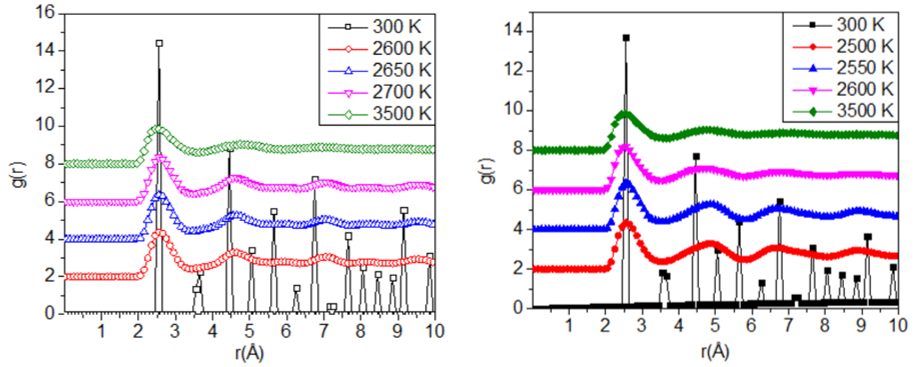


a) RDF of crystals Cr at different temperature b) RDF of polycrystals Cr at different temperature

***Figure 5***. Radial distribution function of the Cr model at different temperatures

Figure 5 presented compares the radial distribution function (RDF), g(r), for chromium (Cr) atoms in both crystal (left) and polycrystal (right) forms at different temperatures (300 K, 2500 K, 2600 K, 2650 K, 2700 K, 3500 K). RDF provides insights into the atomic structure by depicting how atomic density varies as a function of distance from a reference atom. For crystal Cr RDF (Figure 5a), at low temperatures (300 K), sharp peaks are visible, indicating a well-ordered structure typical of crystalline solids. As the

temperature increases, the peaks become broader, and their intensity reduces, particularly at temperatures above 2600 K, suggesting the onset of melting. At 3500 K, the RDF flattens, which indicates a liquid state where long-range order disappears, though short-range order (nearest neighbors) remains. In polycrystal Cr RDF (Figure 5b), similar to the crystal form, at low temperatures (300 K), distinct peaks appear, although slightly broader compared to the crystal, due to the inherent structural imperfections of polycrystals. The melting transition is observed at a lower temperature (~2480 K), as evident from the more rapid decrease in peak intensity between 2500 K and 2700 K. At 3500 K, the RDF again flattens, confirming the complete transition to a liquid state.

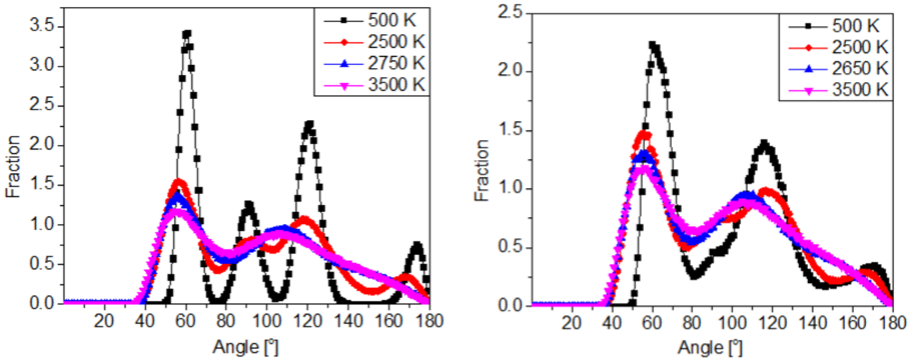


a) Angle distribution of crystal Cr at different temperature

b) Angle distribution of polycrystal Cr at different temperature

***Figure 6***. Angle distribution of crystal and polycrystal models at different temperatures

Figure 6a and Figure 6b display the angle distribution between the crystal and polycrystal models at various temperatures. At low temperatures (500 K), both samples exhibit a pronounced angle distribution with significant peaks, indicating the ordered arrangement of Cr atoms. However, as the temperature increases (from 2500 K to 3500 K), the distribution becomes more uniform, reflecting the breakdown of ordered structures and the onset of phase transition. The angle distribution in the crystal model maintains a more orderly structure compared to the polycrystal model as the temperature rises. Nonetheless, both models show a trend toward disorder as the material begins to melt. Thus, the crystal exhibits a higher melting temperature and density, reflecting a more stable structure compared to the polycrystal.

Figure 7 illustrates the Mean Square Displacement (MSD) of Cr atoms in both crystal and polycrystal models at different temperatures. Figure 7a shows MSD of Cr atoms in the crystal model. MSD shows a gradual increase in the displacement of Cr atoms over time at various temperatures (from 300 K to 3500 K). At lower temperatures like 300 K, the atomic displacement is smaller, resulting in a lower MSD, indicating that atoms remain more localized, typical of the solid phase. As the temperature rises (from 2500 K to 3500 K), the slope of the MSD curve becomes steeper, signifying an increase in atomic thermal motion. This can be explained by atoms overcoming energy barriers and transitioning towards a liquid state. Figure 7b displays MSD of Cr atoms in the polycrystal model. Similar to the crystal model, the MSD increases over time and with temperature. However, the MSD curves for the polycrystal model differ from those of the crystal model. At the same temperature, atoms in the polycrystal model tend to move more than those in the crystal model, especially at higher temperatures. This reflects that the polycrystal structure may be less stable, leading to more significant atomic displacement

under high-temperature conditions. Therefore, both models indicate that as the temperature increases, the motion of Cr atoms increases significantly, especially at temperatures near the melting point, demonstrating higher diffusion and a phase transition from solid to liquid.

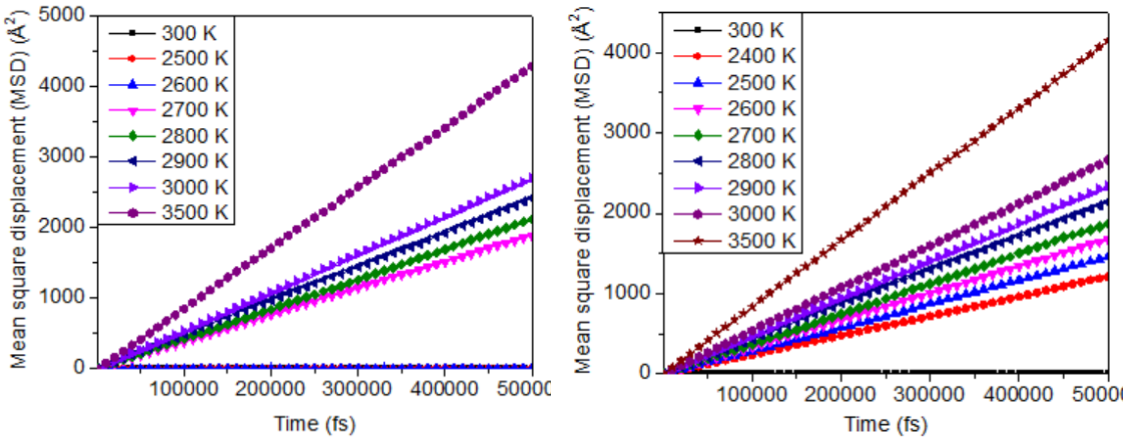


a) MSD of Cr atoms in the crystal model b) MSD of Cr atoms in the polycrystal model

***Figure 7***. Mean square displacement of Cr atoms in the crystal and polycrystal models

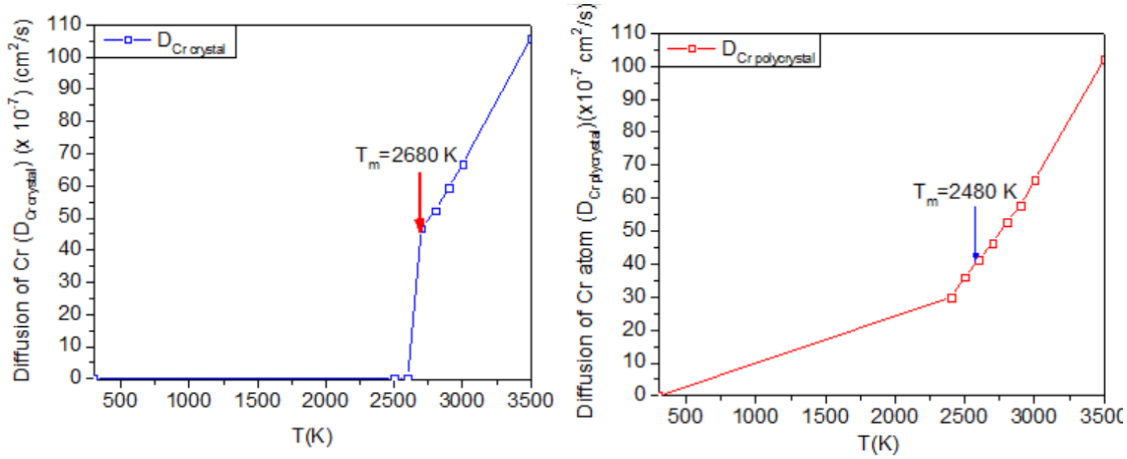


a) D of Cr atoms in the crystal model b) D of Cr atoms in the polycrystal model

***Figure 8***. Diffusion coefficient of Cr atoms in the crystal and polycrystal models

Figure 8 presents the diffusion coefficient D of Cr atoms in two models: the crystal model (on the left) and the polycrystal model (on the right). The diffusion coefficient is shown as a function of temperature from 500 K to 3500 K. Figure 8a shows the diffusion coefficient D of Cr atoms in the crystal model as a function of temperature. At lower temperatures (below the melting temperature $T_m$=2680 K), the diffusion coefficient remains near zero, indicating minimal atomic mobility. Once the system reaches the melting point of 2680 K, there is a sharp increase in D, signifying a phase transition to a liquid state where atoms gain significant mobility. Above the melting temperature, the diffusion coefficient rises steeply, indicating that the atoms are more mobile due to the higher kinetic energy in the liquid phase. For the polycrystal model (Figure 8b), a similar behavior is observed with the diffusion coefficient remaining low until the material reaches the melting temperature $T_m$=2480. After this temperature, the diffusion

coefficient increases sharply, signaling a phase transition. However, the transition occurs at a lower temperature compared to the crystal model. Above 2480 K, the diffusion in the polycrystal system increases as the material transitions to the liquid phase, similar to the crystal model, but at a slightly lower temperature due to the polycrystalline structure. Thus, the melting point for the polycrystal model ($T_m$=2480 K) is lower than that of the crystal model ($T_m$=2680 K), indicating that the polycrystal melts earlier. This difference in melting temperatures can be attributed to the grain boundaries and defects present in the polycrystalline structure, which serve as preferential sites for atomic mobility and phase transition.

## 4. Conclusion

Models of crystalline and polycrystalline Cr are constructed using molecular dynamics simulations. The simulated results are analyzed through the total energy function, heat capacity, radial distribution function, and angle distribution. It has been indicated by observations that the melting temperature of crystalline Cr is higher than that of polycrystalline Cr, demonstrating that polycrystalline structures are less thermally stable than their crystalline counterparts, with earlier phase transitions. Dynamics are evaluated through the analysis of the mean squared displacement and diffusion coefficient. The role of crystallinity in diffusion behavior and phase transitions is highlighted by the findings, with enhanced atomic mobility at lower temperatures exhibited by polycrystalline material compared to the crystal structure. Material applications involving high-temperature environments are considered important in light of these results. Studying the mechanical properties of Cr materials is of great importance; in our future research, we will investigate the mechanical characteristics of these materials by molecular dynamics.

***Acknowledgment***

*Our results have been calculated by using the High-Performance Computing (HPC) server at Thu Dau Mot University, Binh Duong Province, Vietnam.*

**References**

Bloom, D. S., & Grant, N. J. (1951). Chromium-nickel phase diagram. *JOM*, 3, 1009-1014.

Bloom, D. S., Putman, J., & Grant, N. (1952). Melting point and transformation of pure chromium. *JOM*, *4*(6), 626-626.

Carlile, S., Christian, J., & Hume-Rothery, W. (1949). The equilibrium diagram of the system chromium-manganese. *J. Inst. Met*, *76*(2), 169-194.

Choi, W.-M., Kim, Y., Seol, D., & Lee, B.-J. (2017). Modified embedded-atom method interatomic potentials for the Co-Cr, Co-Fe, Co-Mn, Cr-Mn and Mn-Ni binary systems. *Computational Materials Science*, 130, 121-129.

Emsley, J. (2011). Nature's building blocks: an AZ guide to the elements: Oxford University Press, USA.

Greenaway, H., Johnstone, S., & McQuillan, M. (1951). High-Temperature Thermal Analysis Using the Tungsten/Molybdenum Thermocouple. *J. Inst. Metals*, 80.

Grube, G., & Knabe, R. (1936). Elektrische Leitfähigkeit und Zustandsdiagramm bei binären

HARADA, H., YAMAZAKI, M., & KOIZUMI, Y. (1979). A Series of Nickel-Base Superalloy on γ-γ′ tie Line of Alloy Inconel 713C. Tetsu-to-Hagane, *65*(7), 1049-1058.

Haworth, C., & Hume-Rothery, W. (1959). The Constitution of Molybdenum-Rhodium and Molybdenum-Palladium Alloys. Appendix: the Construction of Two Laboratory Furnaces for Use Above 2000° C. *J. Inst. Metals*, 87.

Hoover, W. G. (1985). Canonical dynamics: Equilibrium phase-space distributions. Physical review A, *31*(3), 1695.

Ioroi, K., Aono, Y., Xu, X., Omori, T., & Kainuma, R. (2022). Melting Point of Pure Cr and Phase Equilibria in the Cr-Si Binary System. Journal of Phase Equilibria and Diffusion, *43*(2), 229-242.

Josell, D., Basak, D., McClure, J., Kattner, U. R., Williams, M. E., Boettinger, W. J., & Rappaz, M. (2001). Moving the pulsed heating technique beyond monolithic specimens: Experiments with coated wires. *Journal of Materials Research*, *16*(8), 2421-2428.

Legierungen.: 21. Mitteilung: Das System Palladium-Chrom. *Zeitschrift für Elektrochemie und angewandte physikalische Chemie*, *42*(11), 793-804.

Long, H., Mao, S., Liu, Y., Zhang, Z., & Han, X. (2018). Microstructural and compositional design of Ni-based single crystalline superalloys—A review. *Journal of Alloys and Compounds*, 743, 203-220.

Nosé, S. (1984). A unified formulation of the constant temperature molecular dynamics methods. The Journal of chemical physics, *81*(1), 511-519.

Perepezko, J. H. (2009). The hotter the engine, the better. Science, *326*(5956), 1068-1069.

Plimpton, S. (1995). Fast parallel algorithms for short-range molecular dynamics. Journal of computational physics, *117*(1), 1-19.

Putman, J., Potter, R., & Grant, N. (1951). The ternary system chromium-molybdenum-iron. TRANSACTIONS OF THE AMERICAN SOCIETY FOR METALS, 43, 824-852.

Reed, R. C. (2008). The superalloys: fundamentals and applications: Cambridge university press.

Senkov, O., Wilks, G., Miracle, D., Chuang, C., & Liaw, P. (2010). Refractory high-entropy alloys. *Intermetallics*, *18*(9), 1758-1765.

Shibuta, Y., & Suzuki, T. (2008). A molecular dynamics study of the phase transition in bcc metal nanoparticles. *The Journal of chemical physics*, *129*(14).

Stukowski, A. (2009). Visualization and analysis of atomistic simulation data with OVITO–the Open Visualization Tool. Modelling and simulation in materials science and engineering, *18*(1), 015012.

Unceta, N., Séby, F., Malherbe, J., & Donard, O. F. X. (2010). Chromium speciation in solid matrices and regulation: a review. Analytical and bioanalytical chemistry, 397, 1097-1111.

Xia, W., Zhao, X., Yue, L., & Zhang, Z. (2020). A review of composition evolution in Ni-based single crystal superalloys. *Journal of Materials Science & Technology*, 44, 76-95.